

Joint Transmission for Cellular Networks with Pinching Antennas: System Design and Analysis

Enzhi Zhou, *Member, IEEE*, Jingjing Cui, *Senior Member, IEEE* and Ziyue Liu,
Zhiguo Ding, *Fellow, IEEE* and Pingzhi Fan, *Fellow, IEEE*

Abstract—As an emerging flexible antenna technology for wireless communications, pinching-antenna systems, offer distinct advantages in terms of cost efficiency and deployment flexibility. This paper investigates joint transmission strategies of the base station (BS) and pinching antennas (PAS), focusing specifically on how to cooperate efficiently between the BS and waveguide-mounted pinching antennas for enhancing the performance of the user equipment (UE). By jointly considering the performance, flexibility, and complexity, we propose three joint BS-PAS transmission schemes along with the best beamforming designs, namely standalone deployment (SD), semi-cooperative deployment (SCD) and full-cooperative deployment (FCD). More specifically, for each BS-PAS joint transmission scheme, we conduct a comprehensive performance analysis in terms of the power allocation strategy, beamforming design, and practical implementation considerations. We also derive closed-form expressions for the average received SNR across the proposed BS-PAS joint transmission schemes, which are verified through Monte Carlo simulations. Finally, numerical results demonstrate that deploying pinching antennas in cellular networks, particularly through cooperation between the BS and PAS, can achieve significant performance gains. We further identify and characterize the key network parameters that influence the performance, providing insights for deploying pinching antennas.

Index Terms—Pinching antennas (PAS), BS-PAS joint transmission schemes, performance analysis

I. INTRODUCTION

The advent of the sixth generation (6G) networks opens up a new venue of revolutionary advancements in mobile communications, for improving communication efficiency and expanding coverage in pervasive communication areas. With this momentum, multiple-input and multiple-output (MIMO) [1] and massive MIMO [2] techniques were deployed to provide high multiplexing gains and space division multiple access, which lays fundamental principles of providing high-speed and large-connectivity transmissions. In order to provide more flexibility for antenna configuration, emerging flexible-antenna techniques, such as reconfigurable intelligent surfaces [3], dynamic metasurface antennas [4], fluid antennas [5], movable antennas [6], pinching antennas (PAS) [7] and among others, have attracted widespread interest from academia and industry. Compared to their peers, the PAS possess a number

of good features, including flexible deployment that enables rapid establishment of mobile communication coverage, low-cost configuration that can be created by applying simple dielectric particles, e.g., clothes pinches on waveguides, and thus pinching antennas have become a promising technique to create strong line-of-sight (LoS) connections quickly and economically [7–9].

When the line-of-sight (LoS) path between base stations (BS) and user equipment (UE) is obstructed, the use of PAS can create alternative LoS channels through waveguide-extended deployment and low-cost PAS, thereby enhancing received signal power at UEs. To this end, this paper focuses on how to design the joint transmission scheme by leveraging both the massive antenna arrays at the BS and the flexible deployment advantages of PAS to achieve superior performance gains.

Motivated by the demonstration from DOCOMO 2022 [7], PAS with the features of fast and cost-effective construction has been viewed as one of propitious flexible antenna technologies to provide seamless coverage that has attracted great research efforts [8] and [10]. The basic design principles for pinching-antenna systems were proposed in [11] from the perspective of practical deployment, in which analytical performance comparisons were conducted by using both conventional orthogonal multiple access and non-orthogonal multiple access (NOMA), respectively. Following this principle, the pinching-antenna locations were optimized by maximizing the sum rate of the system [12], where multiple PAS were deployed on a single waveguide to serve a single user. The array gain of pinching-antenna systems was investigated in [13] with respect to the number of PAS and the inter-antenna spacing. As a further advance, NOMA assisted pinching-antenna systems with multiple waveguides and each having a single pinching antenna in [14].

For uplink pinching-antenna systems, the sum rate maximization problem also have attracted a lot of research interest in different scenarios [15–17]. More explicitly, the sum rate was optimized concerning the position of PAS and the power allocation of the users for a pinching-antenna assisted NOMA system with one waveguide and one pinching antenna. [16] considered an uplink pinching-antenna assisted multiuser multiple input single-output (MISO) system with multiple waveguides and each having one pinching antenna, in which the sum rate was maximized by designing the power of the users and the positions of the PAS on each waveguide. In [17], a pinching-antenna system with multiuser multiple-input multiple-output (MIMO) was considered, where the digital precoding matrix and the location of the PAS on each waveguide were jointly designed to maximize a weighted sum

E. Zhou and Z Liu are with the Department of Computer and Software Engineering, Xihua University, Sichuan, China (e-mail: ezhou@mail.xhu.edu.cn, liuziyue_2006@126.com).

J. Cui and P. Fan are with the School of Information Science and Technology, Southwest Jiaotong University, Chengdu 610031, China (e-mail: jingjing.cui@swjtu.edu.cn; p.fan@ieec.org).

Z. Ding is with the Department of Computer and Information Engineering, Khalifa University, Abu Dhabi, UAE, and the Department of Electrical and Electronic Engineering, the University of Manchester, Manchester, UK. (e-mail: zhiguo.ding@manchester.ac.uk).

rate.

Due to their superior comparability, PAS can be applied to various communication systems. For example, [18] considered the physical-layer security system with PAS, which demonstrates that the secrecy capacity between the base station and the legitimate user increases when the height of the pinching-antenna is closer to the user. Furthermore, the application of PAS to covert communications was explored in [19]. Another appealing direction is to explore the benefits of how to use PAS to support integrated sensing and communications [20, 21] in terms of the Cramér–Rao lower bound (CRLB). Considering the low-cost and flexible reconfigurability features of PAS, [20] firstly derived the CRLB of the pinching-antenna assisted integrated sensing and communication (ISAC) systems, revealing the potential benefits in realizing flexible user-centric positioning. More sophisticated research work has been recently conducted in [21–23] for further exploring the benefits of PAS in ISAC systems.

We note that PAS can be treated as a distributed-antenna system [24] with PAS distributed on spatially separated waveguides that are connected to the BS via an interface unit. Distributed-antenna systems were originally proposed to cover the coverage dead spots in indoor communications [25], and design specifications of distributed-antenna systems were further provided in [26]. Therefore, it is possible that the joint transmission scheme can leverage both the massive antenna arrays at BS and the flexible deployment advantages of PAS to achieve superior performance gains. Similar to cooperative reconfigurable intelligent surface (RIS) systems, where the phase shifts of RIS elements were designed to manipulate reflected signals [27], the BS-PAS system achieves efficient joint transmission by appropriately designing the phases of signals transmitted from the PAS. However, cooperative transmission between the BS and the PAS typically requires the exchange of channel state information (CSI) and joint baseband processing [28]. Since the multi-antenna BS and the PAS operate independently at the baseband, enabling joint signal processing would inevitably lead to increased system complexity. Consequently, the deployment of the PAS in existing cellular networks should minimize modifications to current baseband and radio frequency (RF) systems. To this end, this paper investigates BS-PAS joint transmission architectures, analyzes their feasibility and trade-offs between the performance and complexity. We propose beamforming designs tailored to various BS-PAS deployment configurations considered in this paper, and conduct a comprehensive performance analysis, providing practical guidelines for integrating PAS into cellular networks. The main contributions of this paper are as follows.

- We propose three BS-PAS joint transmission schemes in terms of the coordination levels of signal processing between the BS and PAS. Based on considerations of communication performance, deployment flexibility, and network complexity, we propose three distinct joint BS-PAS transmission architectures: standalone deployment (SD), semi-cooperative deployment (SCD) and full-cooperative deployment (FCD).
- We design the optimal beamforming vectors based on the

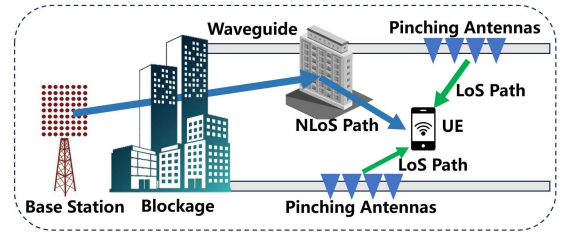


Fig. 1. The joint transmission scenario of the BS and PAS.

maximum ratio transmission (MRT) principle, tailored to each of the three proposed joint transmission schemes. In particular, we analyze how the design of pinching-antenna positions facilitates the derivation of the corresponding beamforming vectors. As coordination among the antennas increases across the SD, SCD and FCD schemes, the system performance improves at the cost of higher implementation complexity.

- We derive closed-form expressions of the average received signal-to-noise ratio (SNR) based on the designed optimal beamforming vectors for each of the three proposed joint BS-PAS transmission schemes. We then analyze the performance gains of three schemes compared to the conventional BS-only approach, providing mathematical expressions in closed-form that quantify the achievable improvements.
- Monte Carlo simulations are conducted to validate the developed results on the average received SNR for the three proposed BS-PAS joint transmission schemes. Our numerical evaluations demonstrate that the three proposed BS-PAS joint transmission schemes achieve substantial performance improvements in most scenarios compared to the conventional BS-only scheme.

II. SYSTEM MODEL AND CHANNEL CHARACTERIZATION

A. System model

In this paper, we consider a downlink pinching-antenna assisted communication scenario as shown in Fig. 1, where the BS equipped with N_B antennas communicates with one single-antenna users with the assistance of PAS. There are K waveguides deployed, with N_G PAS activated on each waveguide. Assume that the LoS path between the BS and the UE is blocked by some obstacles. As a result, the user equipment receives the transmitted signals from the BS via NLoS propagation and from the PAS via LoS paths, which requires the cooperative transmission by the BS and PAS.

B. Channel characterization

Following [7], the channel between a waveguide-mounted pinching antenna and the UE can typically be characterized as a LoS channel. To evaluate the impact of different propagation environments between the BS-UE and PAS-UE channels, we employ distinct path loss exponents to capture these different channel characteristics [29].

a) *BS-UE channel model*: The channel between the BS and the UE can be represented as

$$\mathbf{h}_B = \sqrt{\frac{\eta}{L_B^\alpha}} \tilde{\mathbf{h}}_B, \quad (1)$$

where $\tilde{\mathbf{h}}_B = [\tilde{h}_{B,1}, \dots, \tilde{h}_{B,N_B}]$ and $\eta = \frac{c^2}{16\pi^2 f_c^2}$. c and f_c are the speed of light and the carrier frequency, respectively. L_B is the distance between BS and the UE and α is the path loss exponent [30], characterizing the rate at which signal power attenuates with propagation distance. Moreover, $\tilde{h}_{B,i} \in \mathbb{C}$ is the channel coefficient between the i -th BS antenna and the UE, which is modeled as the Rayleigh fading channel, where the amplitude of channel gain $|\tilde{h}_{B,i}|$ follows a Rayleigh distribution with scale parameter $\sigma^2 = \frac{1}{2}$, i.e., $|\tilde{h}_{B,i}| \sim \text{Rayleigh}(\frac{1}{\sqrt{2}})$.

b) *PAS-UE channel model*: Let $\varphi_{f,k}$ denote the coordinate of the signal injection point for waveguide k , while $\varphi_{k,n}$ represents the coordinate of the n -th pinching antenna on waveguide k . Assume that the UE is located at position φ_u . The phase delay experienced by the signal injected into waveguide k when propagating through the n -th pinching antenna to reach the UE can be expressed as

$$\psi_{k,n} = \frac{2\pi}{\lambda} \|\varphi_{k,n} - \mathbf{u}\| + \frac{2\pi}{\lambda_G} \|\varphi_{k,n} - \varphi_{f,k}\|, \quad (2)$$

where $\lambda = \frac{2\pi}{f_c}$ is the wavelength in the free space, $\lambda_G = \frac{\lambda}{n_{eff}}$ represents the wavelength of the signal within the waveguide, and n_{eff} denotes the effective refractive index of the dielectric waveguide.

Following the results in [12], the positions for PAS are assumed to be consistently clustered at the location closest to the UE along the waveguide, requiring only wavelength-level fine tuning of the antenna positions to achieve the maximum antenna gain. Since the signal wavelength in the band of wireless cellular networks is typically less than 100 millimeters, such positional adjustments has a negligible affect on the large-scale path loss. Additionally, we neglect the transmission loss inside the waveguide as in [10]. Thus, the PAS-UE channel through the k -th waveguide is given by

$$\begin{aligned} h_{G,k} &= \frac{\sqrt{\eta}}{\|\varphi_{k,n} - \mathbf{u}\|} \times \sqrt{\frac{1}{N_G} \sum_{n=1}^{N_G} e^{-j\psi_{k,n}}} \\ &= \sqrt{\frac{\eta}{L_{G,k}^\beta N_G}} \sum_{n=1}^{N_G} e^{-j\psi_{k,n}}, \end{aligned} \quad (3)$$

where $L_{G,k}$ is the distance between PAS on the k -th waveguide and the UE, and β is the associated path loss exponent. Thus, $L_{G,k}^\beta$ represents the path loss between PAS on the k -th waveguide and the UE. Moreover, we consider that each antenna at the BS is equipped with a dedicated RF chain, whereas each waveguide – despite containing multiple PAS – is served by a single RF chain. Consequently, the joint downlink channel of the UE from the BS and PAS can be modeled as a MISO channel with a total of $N_B + K$ transmit antennas.

III. PROPOSED BS-PAS JOINT TRANSMISSION SCHEMES

In this section, we start by introducing the three proposed joint transmission schemes, categorized according to the level of cooperation between the BS and PAS. This is followed by an analysis of the optimal deployment of PAS on each waveguides, which in turn motivates the use of a joint transmission

channel model for the BS-PAS cooperative system, serving as the foundation for designing optimal beamforming vectors.

A. Proposed joint transmission schemes

Inspired by the specification of distributed-antenna system [26], we treat pinching-antenna systems with multiple waveguides as a cooperative infrastructure in this paper, which can be operated in three different manners: 1) the BS signal distributes the signal to separate waveguide processing units (WPUs) that can be deployed in different locations, in which each WPU independently feeds the signal to PAS on each waveguide (e.g., optical fiber cables or dedicated structured cabling) for improving the communication performance and coverage of the system; 2) the signal transmit from the BS is connected to a common WPU that is deployed in some place different from the BS, which then distributed the signal to each waveguide simultaneously; 3) the WPU is integrated in the BS, in which the BS signal is fed to the waveguides directly from the BS without further intermediate interface. Correspondingly, three BS-PAS joint transmission deployment architectures are developed: standalone deployment, semi-cooperative deployment, and joint deployment. The three joint transmission architectures are illustrated in Fig. 2.

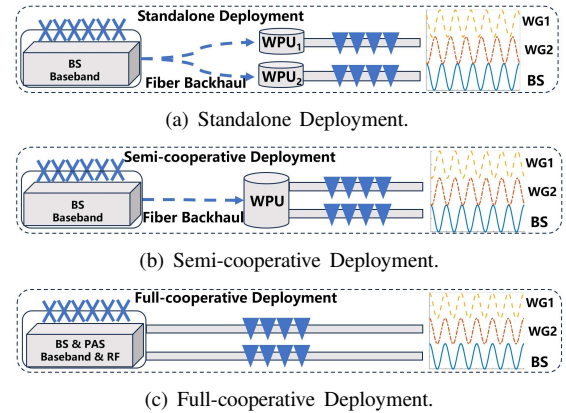


Fig. 2. The architectures of BS-PAS joint transmission system.

a) *Standalone deployment (SD)*: In the SD scheme, as shown in Fig. 2(a) with two waveguides: WG1 and WG2, it places separate waveguide processing units (WPUs) in different service areas, connected to the BS via optical fibers. This architecture offers maximum deployment flexibility of PAS while reducing power loss and interference risks from long-distance waveguide transmission. In this scheme, each WPU needs to obtain UE location information and baseband signals from the BS, then adjusts its pinching-antenna positions to generate and inject radio-frequency signals into the waveguide. Each waveguide independently adjusts its PAS, resulting in phase differences of the received signals from different waveguides and BS, as shown in Fig. 2(a).

b) *Semi-cooperative deployment (SCD)*: As shown in Fig. 2(b), in the SCD scheme, the processing units of all waveguides are co-located, allowing for joint signal processing among all PAS. Here, the centralized WPU enables power allocation among different waveguides. Additionally, multiple waveguides can coordinately adjust pinching-antenna positions

to ensure in-phase signal superposition at the receiver for the maximum array gain of PAS. However, this enhanced coordination comes at the cost of reduced PAS deployment flexibility. Compared to the SD scheme, the joint WPU in SCD enables joint adjustments of PAS to achieve signal-phase alignment across all waveguides, resulting in increased WPU complexity.

c) Full-cooperative deployment (FCD): In the FCD scheme, the WPUs are incorporated into the BS, facilitating fully joint signal processing across the BS and all PAS. This enables flexible power allocation between the BS antennas and waveguides, as well as coordinated placement of PAS, thereby achieving maximum beamforming gain. Nevertheless, the FCD scheme requires significant modifications to existing BS baseband processing, and waveguide routing from the BS reduces the flexibility of PAS while increasing deployment costs. Moreover, full cooperation between the BS and waveguides introduces additional challenges in the placement and configuration of PAS. Due to the non-idealities of oscillators and antennas, the transmitted signal typically experiences phase noise, which can be estimated at the receiver using demodulation reference signals (DMRS) and subsequently pre-compensated at the transmitter [31, 32]. This implies that in order to ensure phase alignment with the BS-transmitted signal, the PAS must dynamically adjust their positions to match the BS signal phase. This requirement introduces additional signal processing complexity and poses potential risk of delayed adjustments for the PAS.

We summarize the features of three joint transmission architectures in Table. I. The coordination levels and implementation complexity are progressively increasing across the three architectures. Therefore, practical network deployment should seek a balance between performance requirements and implementation complexity by selecting the most appropriate architecture.

TABLE I

CHARACTERISTICS OF DIFFERENT JOINT TRANSMISSION ARCHITECTURES

Architectures	Deployment flexibility	Implementation complexity	Signal coordination level
SD	High	Low	Non-coherent
SCD	Medium	Medium	Partial coherent
FCD	Low	High	Ideal coherent

B. The joint BS-PAS channel

Let $\varphi_{k,1}$ and $\psi_{k,1}$ denote the position and the induced phase of the reference pinching antenna on the k -th waveguide, respectively. This reference pinching antenna serves as the phase alignment anchor for determining the position of the remaining PAS on the same waveguide. More specifically, the positions of the remaining PAS can be identified to satisfy the phase coherence condition, thereby ensuring constructive signal combination at the UE [12, 33]. Specifically, for $n = 2, \dots, N_G$, there exists an integer \tilde{k}_n such that the following condition holds.

$$\begin{aligned} & \frac{2\pi}{\lambda} \|\varphi_{k,n} - \mathbf{u}\| + \frac{2\pi}{\lambda_G} \|\varphi_{k,n} - \varphi_{f,k}\| \\ &= \frac{2\pi}{\lambda} \|\varphi_{k,1} - \mathbf{u}\| + \frac{2\pi}{\lambda_G} \|\varphi_{k,1} - \varphi_{f,k}\| + 2\tilde{k}_n\pi, \tilde{k}_n \in \mathbb{Z}. \end{aligned} \quad (4)$$

In this case, the waveguide can be abstracted as an RF port, and the equivalent channel from waveguide RF port k to the UE can be expressed as

$$h_{G,k} = \sqrt{\frac{\eta}{L_{G,k}^\beta N_G}} \sum_{n=1}^{N_G} e^{-j(\psi_{k,1} + 2k_n\pi)} = \sqrt{\frac{\eta N_G}{L_{G,k}^\beta}} e^{-j\phi_k}, \quad (5)$$

where $\phi_k = \psi_{k,1}$ represents the phase delay of the signal transmitted through the reference antenna of the k -th waveguide and arriving at the UE. Next, we give a vanilla example for clarity.

Example 1. Consider a dense urban scenario, to ensure coverage for the UE whose LoS channel from the BS is obstructed by buildings, two waveguides are strategically deployed on the facades of opposing buildings. The UE is assumed to be on the ground at position $(30, 5, 0)$. The feed point positions of the two waveguides are set to $\varphi_{f,1} = (0, 0, 10)$ and $\varphi_{f,2} = (0, 30, 10)$, respectively. The coordinates of the reference PAS are $\varphi_{1,1} = (20, 0, 10)$ and $\varphi_{2,1} = (20, 30, 10)$, respectively. Let $f_c = 3.5$ GHz and $n_{eff} = 1.5$. The corresponding phase anchors of the two waveguides can then be calculated as $\phi_1 = 2.748$ and $\phi_2 = 0.846$, respectively.

By combining (1) and (5), the aggregate channel from both the BS and pinching antennas to the UE can be expressed as

$$\mathbf{h} = \left[\sqrt{\frac{\eta}{L_B^\alpha}} \tilde{\mathbf{h}}_B, \sqrt{\frac{\eta N_G}{L_{G,1}^\beta}} e^{-j\phi_1}, \dots, \sqrt{\frac{\eta N_G}{L_{G,K}^\beta}} e^{-j\phi_K} \right]. \quad (6)$$

We will evaluate the performance of beamforming schemes using the average received SNR. The received signal can be expressed as

$$\mathbf{y} = \mathbf{h}\mathbf{w}s + \omega, \quad (7)$$

where $\omega \sim \mathcal{C}(0, \sigma_n^2)$ is white complex Gaussian noise with variance σ_n^2 . s and \mathbf{w} are the power normalized transmitted symbol and beamforming vector, respectively, i.e., $|s|^2 = 1$ and $\|\mathbf{h}\|^2 = 1$. Assuming that the total transmit power is P_t , the average received SNR is given by

$$\gamma = \frac{E\{|\mathbf{h}\mathbf{w}|^2\} P_t}{\sigma_n^2}, \quad (8)$$

where $|\mathbf{h}\mathbf{w}|^2$ is the channel gain, which is determined by different BS-PAS architectures and their beamforming schemes.

IV. PROPOSED BEAMFORMING SCHEMES AND PERFORMANCE ANALYSIS

In this section, we first investigate the power allocation schemes among RF ports between the BS and waveguides under three BS-PAS joint transmission architectures to facilitate the derivation of beamforming vectors for each scheme. Subsequently, we present the corresponding beamforming designs for these three architectures and derive the expressions in closed-form in terms of equivalent channels and average SNR at the receiver side.

TABLE II
POWER COEFFICIENTS FOR DIFFERENT JOINT BS-PAS TRANSMISSION
SCHEMES

Architectures	Power Allocation
SD	$P_{S,B} = \frac{N_B}{N_B+K}$ for BS, $P_{S,G} = \frac{1}{N_B+K}$ for each waveguide
SCD	$P_{C,B} = \frac{N_B}{N_B+K}$ for BS, $P_{C,G} = \frac{K}{N_B+K}$ for all waveguides
FCD	Dynamic power allocation among the $N_B + K$ RF chains

A. Power Allocation Scheme Between the BS and Waveguides

In practical implementation, the power allocation flexibility of joint BS-PAS transmission is restricted by the physical deployment and information sharing. In this paper, the power coefficients are used to quantify the proportion of transmit power allocated to the BS and PAS relative to the total power budget.

As discussed in Section II, each BS antenna and each waveguide corresponds to one RF chain. Thus, there are $N_B + K$ RF chains in total in the BS-PAS joint transmission system. To ensure consistency in the total transmit power, in SD and SCD schemes, power allocation across the BS and waveguides is performed based on the proportions of their RF chains, i.e., $P_{C,B} = \frac{N_B}{N_B+K}$ and $P_{C,G} = \frac{K}{N_B+K}$. In the SD scheme, the channel condition of each waveguide is not shared, then each waveguide receive an equal fraction of the power given to PAS. In the SCD scheme, all waveguides engage in joint channel processing, necessitating a coordinated power allocation among waveguides according to their CSI. In the FCD scheme, the BS and PAS perform joint signal processing, and have the ability to flexibly allocate power among $N_B + K$ RF chains based on the full CSI from BS antennas/pinching antennas to the UE. The power coefficients of joint transmission architectures are shown in Table. II. Following the predefined power allocation strategy as discussed above, we will investigate the optimal beamforming schemes for each transmission strategy, respectively, in the following section.

B. Beamforming design for the SD scheme

Through uplink channel estimation and leveraging the channel reciprocity between uplink and downlink, the optimal downlink beamforming vector at the BS is maximum ratio transmission (MRT) [31]. Incorporating the power coefficients, the optimal beamforming vector at the BS can be expressed as

$$\tilde{\mathbf{w}}_B = \sqrt{P_{S,B}} \frac{\mathbf{h}_B^H}{\|\mathbf{h}_B^H\|} = \sqrt{\frac{P_{S,B}}{\|\tilde{\mathbf{h}}_B\|^2}} \tilde{\mathbf{h}}_B^H, \quad (9)$$

where each waveguide can adjust the positions of its own N_G pinching antennas. Since the WPU of each waveguide are independently deployed, joint power allocation cannot be implemented. Therefore, equal power allocation is adopted among different waveguides. Consequently, under the SD scheme, the beamforming vector of the waveguide transmission only fed the modulated symbols into the waveguide at

a given transmit power. Combined with the BS's precoding vector, the power normalized beamforming vector for the SD scheme can be expressed as a $N_B + K$ vector

$$\mathbf{w}_S = \left[\sqrt{\frac{P_{S,B}}{\|\tilde{\mathbf{h}}_B\|^2}} \tilde{\mathbf{h}}_B^H, \sqrt{P_{S,G}}, \dots, \sqrt{P_{S,G}} \right]. \quad (10)$$

In this context, the power allocation among the antennas at the BS is conducted within beamforming, but no power allocation is implemented between the BS and the PAS, or among the waveguides themselves.

Based on the joint channel in (6), the channel observed at the UE can be expressed as

$$\begin{aligned} h_S &= \mathbf{h} \mathbf{w}_S \\ &= \sqrt{\frac{\eta P_{S,B}}{L_B^\alpha}} \|\tilde{\mathbf{h}}_B\| + \sqrt{\eta N_G P_{S,G}} \sum_{k=1}^K \sqrt{\frac{1}{L_{G,k}^\beta}} e^{-j\phi_k}. \end{aligned} \quad (11)$$

In the equation, $\sum_{k=1}^K \sqrt{\frac{1}{L_{G,k}^\beta}} e^{-j\phi_k}$ is determined by the reference antennas of each waveguide and the UE's position. It can be observed that the equivalent channels from different waveguides may combine constructively when in-phase, or destructively when out-of-phase, at the receiver. When destructive cancellation occurs, the received waveguide signal power at the UE will decrease. Moreover, if the direction of $\sum_{k=1}^K \sqrt{\frac{1}{L_{G,k}^\beta}} e^{-j\phi_k}$ approaches the negative real axis, the signals from PAS and BS will interfere destructively with each other.

Proposition 1. *The average channel gain for the SD scheme is given by*

$$E \left\{ |h_S|^2 \right\} = \frac{\eta N_B^2}{L_B^\alpha (N_B + K)} + \frac{\eta N_G}{(N_B + K)} \sum_{k=1}^K \frac{1}{L_{G,k}^\beta}, \quad (12)$$

if ϕ_k , the channel phase between the reference pinching antenna and the UE, follows a uniform distribution from 0 to 2π .

Proof. The proof is provided in Appendix A. \square

According to (8), the average received SNR of SD is given by

$$\gamma_{SD} = \frac{\eta N_B^2 P_t}{L_B^\alpha (N_B + K) \sigma_n^2} + \frac{\eta N_G P_t}{(N_B + K) \sigma_n^2} \sum_{k=1}^K \frac{1}{L_{G,k}^\beta}. \quad (13)$$

C. Beamforming design for the SCD scheme

In the SCD scheme, the WPUs can cooperate with each other. Thus, the system can jointly optimize the positions of PAS on each waveguide, ensuring that the signals transmitted from the K waveguide RF ports constructively combine in-phase at the UE. Moreover, power allocation among the waveguides can also be optimized jointly. Without loss of generality, the reference antenna position of the first waveguide is assumed to remain fixed, while the reference antenna positions on the remaining $K - 1$ waveguides are adjusted to align their phase delays in (6) with that of the first waveguide.

Explicitly, suppose that ϕ_1 denotes the phase delay of the first waveguide's signal. Consequently, the reference pinching-antenna position $\varphi_{k,1}$, $k = 2, \dots, K$ can be tuned to satisfy

$$\begin{aligned} & \frac{2\pi}{\lambda} \|\varphi_{k,1} - \mathbf{u}\| + \frac{2\pi}{\lambda G} \|\varphi_{k,1} - \varphi_{f,k}\| \\ & = \phi_1 + 2\tilde{k}\pi, \quad \tilde{k} \in \mathbb{Z}. \end{aligned} \quad (14)$$

Invoked by the bidirectional search concept, an adjustment scheme performs leftward and rightward searches centered around the existing reference antenna position to identify the nearest positions satisfying (14), denoted by $\tilde{\varphi}_{k,1}^L$ and $\tilde{\varphi}_{k,1}^R$. Then the new waveguide positions are determined by

$$\tilde{\varphi}_{k,1} = \begin{cases} \tilde{\varphi}_{k,1}^R & |\tilde{\varphi}_{k,1}^L - \varphi_{k,1}| \geq |\tilde{\varphi}_{k,1}^R - \varphi_{k,1}| \\ \tilde{\varphi}_{k,1}^L & |\varphi_{k,1}^L - \varphi_{k,1}| < |\tilde{\varphi}_{k,1}^R - \varphi_{k,1}|. \end{cases} \quad (15)$$

Following the vanilla example in **Example 1**, we provide an concrete example in **Example 2** for illustrating the optimized positions of the PAS in the proposed system.

Example 2. Referring to the previous example, the search method will adjust the position of the reference antenna for Waveguide 2 to $\tilde{\varphi}_{2,1} = (20.017, 30, 10)$, thus enabling Waveguide 2 to have the same phase delay as Waveguide 1, i.e., in $\phi_1 = \phi_2 = 2.748$. Note that the positions of the remaining antennas in Waveguide 2 also need to be adjusted accordingly to satisfy condition (4).

Furthermore, regarding the power allocation ratios among waveguides, we have the following proposition.

Proposition 2. Given that the reference antenna position on each waveguide satisfies the condition in (14), the maximum equivalent channel gain can be achieved when the power allocation ratio of waveguide k is proportional to its channel gain $\frac{\eta N_G}{L_{G,k}^\beta}$.

Proof. The proof is provided in Appendix B. \square

As cooperation only happens among the waveguides, the MRT transmission for the BS is still the optimal beamforming scheme, and thus the joint beamforming vector in this case can be expressed as

$$\begin{aligned} \mathbf{w}_C = & \left[\sqrt{\frac{P_{C,B}}{\|\tilde{\mathbf{h}}_B\|^2}} \tilde{\mathbf{h}}_B^H, \sqrt{\frac{P_{C,G}}{\sum_{k=1}^K \frac{\eta N_G}{L_{G,k}^\beta}}} \left[\sqrt{\frac{\eta N_G}{L_{G,1}^\beta}}, \dots, \sqrt{\frac{\eta N_G}{L_{G,K}^\beta}} e^{-j(\phi_1 - \phi_K)} \right] \right] \end{aligned} \quad (16)$$

It should be pointed out that unlike conventional beamforming methods, the beamforming for PAS is implemented by configuring the phase $\phi_1 - \phi_k$, which is achieved by adjusting the position of reference pinching antenna on the k -th waveguide.

Therefore, in the SCD scheme, the equivalent channel at the receiver side can be expressed as

$$\begin{aligned} h_C & = \mathbf{h} \mathbf{w}_C \\ & = \sqrt{\frac{\eta P_{C,B}}{L_B^\alpha}} \|\tilde{\mathbf{h}}_B\| + \sqrt{\eta P_{C,G} \sum_{k=1}^K \frac{N_G}{L_{G,k}^\beta}} e^{-j\phi_1}, \end{aligned} \quad (17)$$

where the equivalent channel gain $\sum_{k=1}^K \frac{N_G}{L_{G,k}^\beta}$ of the PAS is determined by both the number of PAS in each waveguide and their distances to the UE, while the equivalent channel phase delay ϕ_1 is governed by the distance between the reference antenna of the first waveguide and the UE. It can be observed that the signals transmitted from the PAS and BS may constructively interfere in-phase at the receiver. However, when the direction of ϕ_1 approaches $\pi + 2\tilde{k}\pi$, they will mutually cancel each other.

Proposition 3. In the SCD scheme, the average channel gain for the SCD scheme has a closed expression as

$$E\{|h_C|^2\} = \frac{\eta N_B^2}{(N_B + K) L_B^\alpha} + \frac{\eta N_G K}{(N_B + K)} \sum_{k=1}^K \frac{1}{L_{G,k}^\beta}. \quad (18)$$

Proof. See Appendix C. \square

Based on the results of **Proposition 3** and the SNR expression in (8), we can obtain the average received SNR of the SCD scheme as follows:

$$\gamma_{SCD} = \frac{\eta N_B^2 P_t}{(N_B + K) L_B^\alpha \sigma_n^2} + \frac{\eta N_G K P_t}{(N_B + K) \sigma_n^2} \sum_{k=1}^K \frac{1}{L_{G,k}^\beta}. \quad (19)$$

D. Beamforming design for the FCD scheme

In the FCD scheme, the BS and all waveguides can perform joint signal processing. In this case, the optimal beamforming vector follows the MRT criterion of the joint channel in (6). For simplicity, we neglect the phase noise of the BS's transmitted signals, and the beamforming vector is given by

$$\begin{aligned} \mathbf{w}_F & = \frac{\mathbf{h}^H}{\|\mathbf{h}\|} \\ & = \frac{\left[\sqrt{\frac{\eta}{L_B^\alpha}} \tilde{\mathbf{h}}_B, \sqrt{\frac{\eta N_G}{L_{G,1}^\beta}} e^{j-\phi_1}, \dots, \sqrt{\frac{\eta N_G}{L_{G,K}^\beta}} e^{j-\phi_K} \right]}{\sqrt{\frac{\eta}{L_B^\alpha} \|\tilde{\mathbf{h}}_B\|^2 + \eta N_G \sum_{k=1}^K \frac{1}{L_{G,k}^\beta}}}, \end{aligned} \quad (20)$$

where the phase shift term $e^{j\phi_k}$ in the k -th waveguide beamforming vector is achieved by tuning the position of the reference pinching antenna in the k -th waveguide. Specifically, based on (4), the position of the reference pinching antenna on the k -th waveguide can be expressed as

$$\begin{aligned} \phi_k & = \left(\frac{2\pi}{\lambda} \sqrt{\|\varphi_{k,1} - \mathbf{u}\|} + \frac{2\pi}{\lambda G} \|\varphi_{k,1} - \varphi_{k,f}\| \right) \\ & = 2\tilde{k}\pi, \quad \tilde{k} \in \mathbb{Z}. \end{aligned} \quad (21)$$

For clarity, we also provide an vanilla example for illustrating the relationship of (21), which is given as follows.

Example 3. Similar to the approach used to satisfy (14), the condition in (21) is fulfilled by performing an antenna position search for each waveguide. Revisiting **Example 1**, we can now determine through this search that the reference antenna on Waveguide 1 is positioned at $\tilde{\varphi}_{1,1} = (19.975, 0, 10)$, while that on Waveguide 2 is located at $\tilde{\varphi}_{2,1} = (19.935, 30, 10)$.

Noting that $\|\tilde{\mathbf{h}}_B\|^2$ is the sum of squares of independent and identical distributed Gaussian random variables, which follows a Gamma Distribution $\Gamma(\nu, \theta)$ with shape parameter $\nu = N_B$ and scale parameter $\theta = \frac{1}{2\sigma^2} = 1$, we have $E\{\tilde{\mathbf{h}}_B\} = N_B$. Following (20), the average transmit power ratio of the BS over multiple fading channel cycles can be obtained as follows:

$$P_{F,B} = \frac{\frac{\eta}{L_B^\alpha} E\left\{\|\tilde{\mathbf{h}}_B\|^2\right\}}{\frac{\eta}{L_B^\alpha} E\left\{\|\tilde{\mathbf{h}}_B\|^2\right\} + \sum_{k=1}^K \frac{\eta N_G}{L_{G,k}^\beta}} = \frac{N_B}{N_B + N_G \sum_{k=1}^K \frac{L_{G,k}^\beta}{L_B^\alpha}}. \quad (22)$$

In this case, the k -th waveguide's average transmit power ratio can also be obtained as follows:

$$P_{F,G,k} = \frac{\frac{\eta N_G}{L_{G,k}^\beta}}{\frac{N_B \eta}{L_B^\alpha} E\left\{\|\tilde{\mathbf{h}}_B\|^2\right\} + \sum_{k=1}^K \frac{\eta N_G}{L_{G,k}^\beta}} \quad (23)$$

$$= \frac{N_G}{N_B \frac{L_{G,k}^\beta}{L_B^\alpha} + N_G \sum_{k'=1}^K \frac{L_{G,k'}^\beta}{L_{G,k}^\beta}}.$$

We can observe from (22) and (23) that the power allocation coefficients assigned to the BS increases as the number of BS antennas grows, i.e., N_B is large, or when the BS is located closer to the UE relative to the PAS on the waveguides of interest, i.e., L_B^α is small. Otherwise, the waveguide will receive higher power allocation than the BS, if it has more PAS than the antennas the BS have, i.e., when N_G is large, or if the PAS are closer to the UE than the BS, i.e., when $L_{G,k}^\beta$ is small.

Now the equivalent channel at the receiver can be expressed as

$$\mathbf{h}_F = \mathbf{h} \mathbf{w}_F = \|\mathbf{h}\|. \quad (24)$$

Therefore, the average channel gain in the full-cooperative scheme is given by

$$E\{|h_F|^2\} = E\left\{\frac{\eta}{L_B^\alpha} \|\tilde{\mathbf{h}}_B\|^2 + \sum_{k=1}^K \frac{\eta N_G}{L_{G,k}^\beta}\right\} \quad (25)$$

$$= \frac{\eta N_B}{L_B^\alpha} + \sum_{k=1}^K \frac{\eta N_G}{L_{G,k}^\beta}.$$

According to (8), the average received SNR of the FCD scheme is

$$\gamma_{FCD} = \frac{\eta N_B P_t}{L_B^\alpha \sigma_n^2} + \sum_{k=1}^K \frac{\eta N_G P_t}{L_{G,k}^\beta \sigma_n^2}. \quad (26)$$

E. Analysis and Discussion

For ease of analysis and comparison, we assume uniform path loss across all waveguide antennas, i.e., $L_{G,k}^\beta = L_G^\beta$. Let $\tilde{\gamma} = \frac{P_t}{\sigma_n^2}$ denote the transmit SNR. Table III summarizes the obtained analytical expression of the average received SNR for different BS-PAS joint transmission schemes. We can see from Table III that the received SNR of BS-PAS joint transmission depends on multiple factors, and the associated performance

TABLE III
AVERAGE RECEIVED SNR OF DIFFERENT SCHEMES

Schemes	Average Received SNR Expression
BS-only	$\gamma_{BO} = \frac{\eta N_B}{L_B^\alpha} \tilde{\gamma}$
BS+PAS SD	$\gamma_{SD} = \left(\frac{\eta N_B^2}{L_B^\alpha (N_B + K)} + \frac{\eta N_G K}{L_G^\beta (N_B + K)} \right) \tilde{\gamma}$
BS+PAS SCD	$\gamma_{SCD} = \left(\frac{\eta N_B^2}{L_B^\alpha (N_B + K)} + \frac{\eta N_G K^2}{L_G^\beta (N_B + K)} \right) \tilde{\gamma}$
BS+PAS FCD	$\gamma_{FCD} = \left(\frac{\eta N_B}{L_B^\alpha} + \frac{\eta N_G K}{L_G^\beta} \right) \tilde{\gamma}$

TABLE IV
JOINT TRANSMISSION GAIN OF SD, SCD AND FCD SCHEMES

Joint Transmission Gain Ratio	Expressions
SD Gain $V_{SD} = \frac{\gamma_{SD}}{\gamma_{BO}}$	$\frac{N_B}{N_B + K} + \frac{N_G K}{N_B (N_B + K)} \frac{L_B^\alpha}{L_G^\beta}$
SCD Gain $V_{SCD} = \frac{\gamma_{SCD}}{\gamma_{BO}}$	$\frac{N_B}{N_B + K} + \frac{N_G K^2}{N_B (N_B + K)} \frac{L_B^\alpha}{L_G^\beta}$
FCD Gain $V_{FCD} = \frac{\gamma_{FCD}}{\gamma_{BO}}$	$1 + \frac{N_G K}{N_B} \frac{L_B^\alpha}{L_G^\beta}$

gains are not guaranteed for all parameter configurations. To this end, we analyze the achievable system gains with respect to different parameter settings.

To facilitate insightful analysis, we introduce the joint transmission gain to quantify the performance improvements of the BS-PAS joint transmission schemes relative to the BS-only scheme. Specifically, it is defined as the ratio of the average received SNR achieved by each of the three BS-PAS joint transmission schemes—SD, SCD, and FCD—to that of the BS-only scheme. Correspondingly, these gains are referred to as the SD gain, SCD gain, and FCD gain, respectively, as shown in Table IV. The analytical expressions for the proposed three schemes are provided in Table IV. In the following analysis, we quantitatively examine the impact of system parameters on the gains of the different transmission schemes. By systematically varying relevant parameters in the gain expressions and analyzing the resulting trends, we can derive the following key insights.

1) *Gains of the proposed joint transmission schemes:* As shown in Table IV, it is evident that the FCD scheme always provides a positive gain of $\frac{N_G K}{N_B} \frac{L_B^\alpha}{L_G^\beta}$ compared to the BS-only scheme, since the FCD Gain $V_{FCD} > 1$ and $\frac{N_G K}{N_B} \frac{L_B^\alpha}{L_G^\beta} > 0$ in BS-PAS joint transmission systems. However, the SD and SCD schemes do not necessarily outperform the BS-only scheme. Their performance advantage depends on specific system parameters, such as the BS-UE path loss exponent α , the number of BS antennas N_B , the number of waveguides K and PAS N_G and among others.

Remark 1. Given $V_{SD} > 1$ and $V_{SCD} > 1$, we have that

- the condition for the SD scheme to outperform the BS-only scheme is $\frac{L_B^\alpha}{L_G^\beta} > \frac{N_B}{N_G}$, whereas
- the SCD scheme achieves gain over the BS-only scheme if $\frac{L_B^\alpha}{L_G^\beta} > \frac{N_B}{N_G K}$.

That is both the SD and SCD schemes outperform the BS-only scheme when $\frac{L_B^\alpha}{L_G^\beta} > \frac{N_B}{N_G}$. To illustrate the performance

gain of SD and SCD schemes compared to BS-only in different scenarios, we provide an example as follows.

Example 4. We use the typical scenario parameter values given in Table V with varying α . From the inequalities $\frac{L_B^\alpha}{L_G^\alpha} > \frac{N_B}{N_G}$ and $\frac{L_B^\alpha}{L_G^\alpha} > \frac{N_B}{N_G K}$, we can compute that $\alpha > 2.13$ and $\alpha > 1.87$, respectively. This indicates that in the considered scenario, the SD scheme outperforms the BS-only scheme when $\alpha > 2.13$, while the SCD scheme always outperforms BS-only scheme as $\alpha \geq 2$.

Example 5. From Remark 1, the conditions under which SD and SCD schemes outperform the BS-only scheme are given by $N_G > \frac{N_B L_G^\beta}{L_B^\beta}$ and $N_G > \frac{N_B L_G^\beta}{K L_B^\beta}$, respectively. Using the typical parameter values given in Table V with $\alpha = \beta = 2$, we obtain the thresholds $N_G > 16$ for the SD scheme and $N_G > 4$ for the SCD scheme, respectively.

2) *Impact of path loss:* We can observe from Table IV that the gains of SD, SCD and FCD schemes over the BS-only scheme monotonically relies on the ratio of the path loss between the BS-UE and the PAS-UE. That is, the gains attained by the proposed transmission schemes grows when the ratio of the path loss, i.e., $\frac{L_B^\alpha}{L_G^\alpha}$, increases. This indicates that cooperation with PAS can provide additional large-scale channel gains.

Remark 2. $V_{FCD} = 1$ when $L_B^\alpha \ll L_G^\beta$, i.e., $\frac{L_B^\alpha}{L_G^\beta}$ goes to 0.

This means that under favorable BS-UE propagation conditions—characterized by a low path loss exponent or short transmission distance—the FCD and BS-only schemes yield comparable performance. In such scenario, the dominant contribution comes from the strong direct BS-UE link.

Remark 3. It should be noticed from Table IV that $\frac{V_{SCD}}{V_{SD}} = K$ and $\frac{V_{FCD}}{V_{SCD}} = 1 + \frac{N_B}{K}$, when $L_B^\alpha \gg L_G^\beta$, i.e., $\frac{L_B^\alpha}{L_G^\beta}$ approaches infinity.

Proof. When $\frac{L_B^\alpha}{L_G^\beta} \rightarrow \infty$, the first term $\frac{N_B}{N_B+K}$ in the expression of V_{SD} and V_{SCD} can be omitted. By dividing V_{SCD} by V_{SD} , we have

$$\lim_{\frac{L_B^\alpha}{L_G^\beta} \rightarrow \infty} \frac{V_{SCD}}{V_{SD}} = \frac{\frac{N_G K^2}{N_B(N_B+K)} \frac{L_B^\alpha}{L_G^\beta}}{\frac{N_G K}{N_B(N_B+K)} \frac{L_B^\alpha}{L_G^\beta}} = K. \quad (27)$$

Furthermore, the first term $\frac{N_B}{(N_B+K)}$ in V_{SCD} and the constant term 1 in V_{FCD} can be omitted if $\frac{L_B^\alpha}{L_G^\beta} \rightarrow \infty$. Similarly, by dividing V_{FCD} by V_{SCD} , we have

$$\lim_{\frac{L_B^\alpha}{L_G^\beta} \rightarrow \infty} \frac{V_{FCD}}{V_{SCD}} = \frac{\frac{N_G K}{N_B} \frac{L_B^\alpha}{L_G^\beta}}{\frac{N_G K^2}{N_B(N_B+K)} \frac{L_B^\alpha}{L_G^\beta}} = 1 + \frac{N_B}{K}. \quad (28)$$

□

The SD scheme processes each waveguide independently, resulting in comparatively lower gains due to the absence of inter-waveguide collaboration. Remark 3 shows that the K -fold gain of the SCD scheme over the SD scheme, which

is achieved through coordination among the K waveguides. Moreover, the performance gain of the FCD scheme over the SCD scheme comes from the additional coordination between the BS and the K waveguides. Since full cooperation in the FCD scheme can avoid allocating power to the BS antennas with poor channel conditions, its the performance gain over the SCD scheme increases with the number of BS antennas.

3) *Impact of the number of BS antennas:* From Table III, it can be observed that since N_B only appears in the numerator of the received SNR for both the BS-only and FCD schemes, their performance improves monotonically as the number of base station antennas increases. However, for the SD and SCD schemes, the two terms of received SNR vary in opposite directions with increasing N_B , resulting in potentially non-monotonic performance behaviors.

Remark 4. As the number of base station antennas approaches infinity, it can be observed from Table IV that V_{SD}, V_{SCD} and V_{FCD} all asymptotically converge to 1. That is, all the three joint transmission schemes achieve the same performance as the BS-only scheme.

In this asymptotic case, nearly all transmit power is allocated to the BS, thereby rendering PAS ineffective. However, the performance of the three joint transmission schemes converge to that of the BS-only scheme at different rates.

Example 6. Using the set of typical scenario parameters in Table V and the gain expression of FCD scheme in Table IV, we can compute that $V_{FCD} \approx 1 + \frac{1224}{N_B}$.

This result indicates that when the number of BS antennas reaches approximately to 1224, the gain of the FCD over the BS-only scheme reduces to 3dB. Therefore, in typical scenarios, the FCD scheme consistently offers substantial performance improvements.

4) *Impact of the number of waveguides:* Now we turn to investigate the impact of the number of waveguides by analyzing the expressions in Table IV. First, as the number of waveguides increases, the performance gain of the joint transmission schemes over the BS-only scheme increase.

Remark 5. As the number of waveguides K approaches infinity, we find that the joint transmission gain becomes $V_{SD} = \frac{N_G L_B^\alpha}{N_B L_G^\beta}$ and $V_{SCD} = V_{FCD} = \frac{K N_G L_B^\alpha}{N_B L_G^\beta}$.

On the one hand, the gain of the SD scheme converges to a constant value, since nearly all power is allocated to PAS, but there is no array gain due to the lack of cooperation among different waveguides. On the other hand, both SCD and FCD schemes achieve gains that increase linearly with the number of waveguides K .

Furthermore, it should be pointed out that as K increases, the received SNR at the UE becomes increasingly dependent on the transmission of PAS. Consequently, the performance of the SCD scheme asymptotically approaches that of the FCD scheme. The performance gain of the FCD scheme over the

SCD scheme can be given by

$$\frac{V_{FCD}}{V_{SCD}} = 1 + \frac{N_B K + N_B K N_G \frac{L_B^\alpha}{L_G^\beta}}{N_B^2 + K^2 N_G \frac{L_B^\alpha}{L_G^\beta}}. \quad (29)$$

Suppose $K = N_B$, then the gain of the SCD scheme over the SCD scheme is $\frac{V_{FCD}}{V_{SCD}} = 2$, i.e., a 3dB improvement. Since the PAS typically are activated on limited waveguides, the FCD scheme generally outperforms the SCD scheme in most practical scenarios.

5) *Impact of the number of PAS*: Finally, we investigate how the number of PAS affects the performance gains of the three proposed joint transmission schemes compared to the BS-only scheme. It can be observed from Table IV that the number of PAS on each waveguide N_G only appears at the numerator of the expression of V_{SD} , V_{SCD} and V_{FCD} , thereby the performance gain of joint transmission schemes over the BS-only scheme increase linearly with N_G .

However, if the number of PAS is small, the expression of received SNR of the SD and SCD scheme may be smaller than 1, that means too few PAS on PAS make the SD and SCD schemes inferior to the BS-only scheme. This is because the waveguide diverts part of the transmit power from BS, but the insufficient number of PAS results in inadequate beamforming gain.

V. SIMULATION RESULTS

In this section, we perform Monte Carlo simulations and numerical evaluations for estimating the performance of the three proposed BS-PAS joint transmission schemes, i.e., SD, SCD, and FCD. For comparison, we consider the conventional BS-only scenario, which serves as the benchmark. In the following simulations, we firstly verify the correctness of our theoretical derivations. Then, we evaluating the achievable gains of the proposed three BS-PAS joint transmission schemes with respect to various system parameters, to offer practical insights practical insights for the design and deployment of future wireless communication networks. Unless otherwise specified, the values of parameters provided in Table V are used throughout the following simulations. In this paper, we consider the typical scenario where the BS-UE path loss is greater than that of the PAS, i.e., the path loss exponents in Table V satisfy $\alpha \geq \beta$. This assumption is due to the fact that the path-loss exponent of an NLoS link is greater than that of an LoS link.

We start by simulating the average SNR received at the UE achieved by the SD, SCD and BS-only schemes. Specifically, in the considered scenario, the BS-UE channel follows a Rayleigh fading model with i.i.d complex Gaussian coefficients $\mathcal{CN}(0, 1)$ with unit variance. The distance between the UE and the BS is set to 200 meters. Suppose that the actual distance between the UE and the reference pinching antenna of a waveguide is randomly generated within the range $[100 - \frac{\lambda}{2}, 100 + \frac{\lambda}{2}]$, ensuring that the phase delay of signals arriving at the UE via PAS on each waveguide follows a uniform distribution over $[0, 2\pi]$.

Fig. 3 shows the average SNR received at the UE versus transmit power for the four different schemes considered. We

TABLE V
SIMULATION PARAMETERS

Parameters	Value
Carrier Frequency	3.5 GHz
Bandwidth	100 MHz
Noise Power Density	-170 dBm/Hz
Transmit Power	1 ~ 100 W (0 ~ 20 dB)
BS-UE Distance	$L_B = 200\text{m}$
RPA-User Distance	$L_G = 100\text{ m}$
Number of BS Antennas	$N_B = 64$
Number of PAS	$N_G = 8$
Number of Waveguides	$K = 4$
Path loss exponents	$\alpha = 2.4, \beta = 2$
Monte Carlo Simulation Number	10000

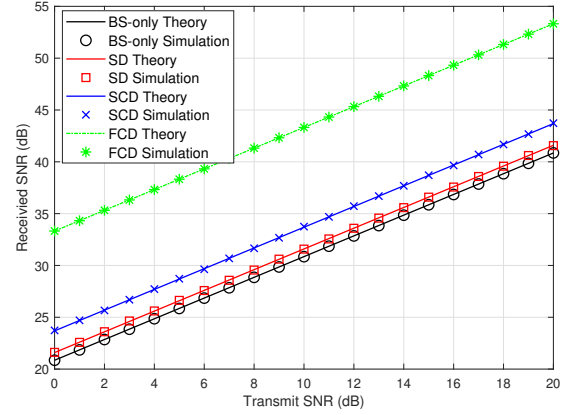


Fig. 3. Average received SNR of different schemes.

see that the simulated SNR matches well with the analytical curves derived in closed-form expressions in (13), (19) and (26). We can also observe from Fig. 3 that the three proposed BS-PAS joint transmission schemes gradually improve the average SNR received at the UE compared to the BS-only scheme, with the FCD scheme achieving the best performance among them. These results follow from the expressions presented in Table III, and further details on how various factors influence the performance gain will be illustrated in the subsequent simulation results.

Fig. 4 shows the impact of the BS propagation environment on the performance of the three proposed joint transmission schemes and their respective gains compared to the BS-only scheme. Here, $\beta = 2$ and the value of α is varied from 2 to 4. This allows us to evaluate how changes in the BS propagation environment influence the performance of the proposed three joint transmission schemes and their gains relative to the BS-only scheme.

We can see from the inset of Fig. 4 that the SD scheme is inferior to the BS-only scheme when the BS-UE path loss exponent falls below 2.13, while the SCD scheme always outperforms the BS-only scheme. This result is consistent with the gain conditions for SD, SCD outlined in Remark 1 and Example 4. Moreover, as the BS-UE path loss exponent continues to decrease, the performance of the FCD and BS-only schemes converges to the same value. This observation is consistent with findings discussed in Remark 2.

We can see from Fig. 4 that the average received SNR of all schemes decreases with increasing the path loss exponent between the BS and the UE. Meanwhile, the FCD scheme

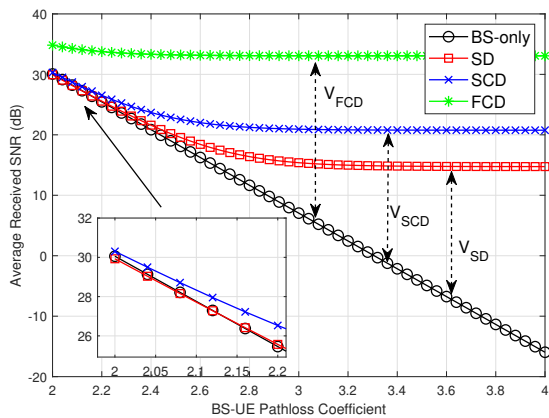


Fig. 4. Average received SNR versus different BS-UE path loss exponents.

consistently attains the best average received SNR compared to the other schemes across the entire range of BS-UE path loss exponents. Moreover, Fig. 4 also shows that the performance gap between the three proposed joint transmission schemes and the BS-only scheme widens as the BS-UE path loss exponent increases. Specifically, the received SNR of the BS-only scheme continuously decreases with increasing the BS path loss exponent, while the three joint transmission schemes converge to fixed performance levels. Furthermore, as the BS-UE path loss coefficient α increases, the additional performance gain of SCD over SD arising from cooperation between different waveguides, and the additional performance gain of FCD over SCD enabled by cooperation between BS and waveguides, will converge to fixed values as described in **Remark 3**.

Fig. 5 illustrates the impact of the number of BS antennas on the received SNR across different schemes, where the number of BS antennas ranges from 1 to 128. We see that the performance of both the BS-only and FCD schemes monotonically increases as the number of BS antennas grows. Nevertheless, as $\alpha > \beta$, the received signal power is primarily dominated by contributions from the PAS. Consequently, the performance of the FCD scheme exhibits a slower rate of improvements as N_B increases compared to the other schemes.

For the SD and SCD schemes in Fig. 5, the received SNR initially decreases and then increases as the number of BS antennas grows. When the BS has a small number of antennas, increasing the number of BS antennas diverts more power away from the PAS, resulting in performance degradation. However, when the number of BS antennas reaches a certain threshold, e.g., 30 for SD and 80 for SCD, the beamforming gain becomes sufficient to compensate for the BS's path loss disadvantage, allowing the SD and SCD schemes to outperform BS-only scheme. Finally, the inset of Fig. 5 shows that the gap between the BS-only, SD and SCD schemes narrows as the number of BS antennas increases, which aligns with the findings in **Remark 4**. Moreover, it can be calculated that the performance gap between the FCD scheme and the BS-only scheme narrows to about 3dB when the number of BS antennas reaches 1224, as shown in **Example 6**.

Fig. 6 demonstrates how the number of waveguides affects the system performance. To illustrate the benefits of employing PAS in different communication scenarios, two different BS-

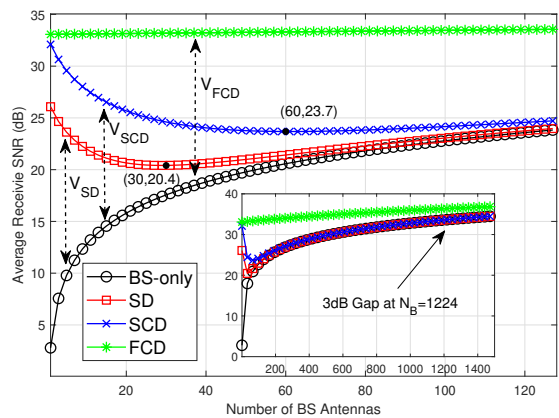


Fig. 5. Average received SNR with different number of BS antennas N_B .

UE path loss exponents, $\alpha = 2.4$ and $\alpha = 2$, are used in Fig. 6(a) and Fig. 6(b), respectively. As shown in Fig. 6(a), all the three proposed joint transmission schemes outperform the BS-only scheme. As the number of waveguides increases, the performance gain of the proposed joint transmission schemes over the BS-only scheme exhibits a rapid initial growth. As the number of waveguides increases further, the gain trends of the three joint transmission schemes begin to diverge. Specifically, the gain of the SD scheme converges to a constant value, while the performance gains of both the SCD and FCD schemes increase monotonically with the number of waveguides K , eventually asymptotically converging to the same level. These results are consistent with the findings in **Remark 5**. In Fig. 6(b), the BS and PAS share the same path loss exponent. The SD scheme demonstrates no gain over BS-only, because $\alpha = 2 < 2.13$ and the condition in **Example 4** is not satisfied. Furthermore, the insets in Fig. 6(b) and Fig. 6(b) illustrates the gain for the FCD scheme over the SCD scheme decreases to 3dB when K increase to 64, i.e., equals to N_B , which are consistent to the analysis under **Remark 5**.

Fig. 7 illustrates the average received SNR performance versus the number of PAS distributed on each waveguide, with two different BS-UE path loss exponents, i.e., $\alpha = 2.4$ and $\alpha = 2$. It shows that the performance gain of joint transmission schemes over the BS-only scheme increase consistently with the number of PAS on each waveguide. Moreover, we can see from the inset in Fig. 7(b) that the SD and SCD schemes initially exhibit poorer performance than the BS-only scheme, since the conditions in **Example 5** are not satisfied. When the number of pinch antennas on each waveguide increases to 16 and 4 for SD and SCD, respectively, that is, conditions in **Example 5** are satisfied, the SD and SCD schemes eventually achieve performance gains.

VI. CONCLUSIONS AND FUTURE WORKS

This paper has investigated joint transmission architectures between BS and PAS, aiming for addressing the deployment challenges of PAS in cellular networks. Specifically, we proposed three different joint transmission schemes, namely SD, SCD and FCD based on the cooperation level between the BS and the PAS. We also developed optimal beamforming schemes based on the MRT principle and derived closed-form expressions of the average received SNR for each transmission

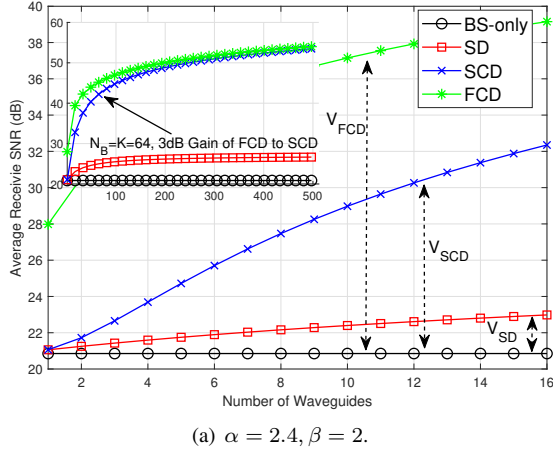
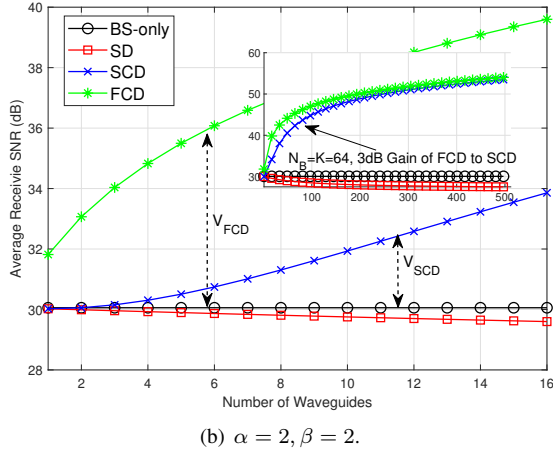
(a) $\alpha = 2.4, \beta = 2$.(b) $\alpha = 2, \beta = 2$.

Fig. 6. Average received SNR versus different numbers of waveguides for different transmission schemes.

strategy. Simulation results were provided to reveal that proposed cooperative transmission strategies between the BS and PAS can significantly enhance communication performance. Moreover, by analyzing the impact of key system parameters, e.g., path loss exponents and the number of PAS, on the transmission efficiency, this work sheds light on the practical deployment of cellular systems integrated with PAS.

Nevertheless, the deployment of PAS in cellular networks presents several key challenges and highlights important directions for future research. For example, efficient coordination between the BS and PAS must be established to support multi-user spatial multiplexing. Additionally, further efforts are needed to reduce the overhead of deploying PAS while minimizing modifications to the existing BS infrastructure. Another key challenge involves joint time-frequency resource scheduling between the BS and PAS. These open issues present promising directions for future research.

APPENDIX A PROOF OF PROPOSITION 1

In this section, we derive the average channel gain for the SD scheme in detail. Since the distance between the reference pinching antenna of each waveguide and the UE is random, we assume that ϕ_k follows a uniform distribution of $[0, 2\pi]$.

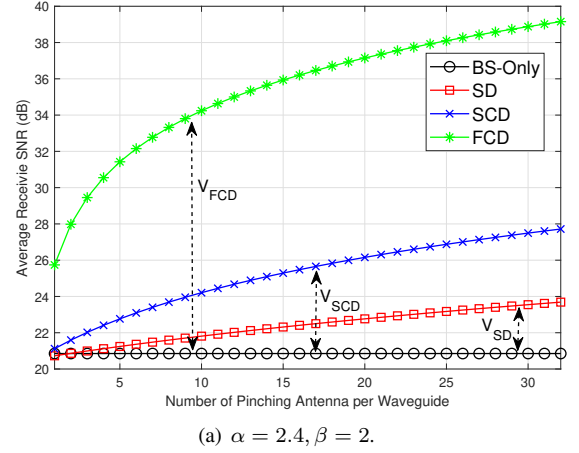
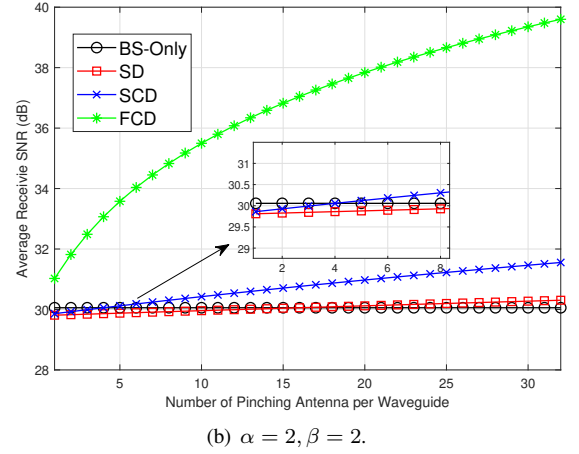
(a) $\alpha = 2.4, \beta = 2$.(b) $\alpha = 2, \beta = 2$.

Fig. 7. Average received SNR with different number of PAS on a waveguide.

For clarity, let

$$Ge^{-j\Omega} = \sum_{k=1}^K \sqrt{\frac{1}{L_{G,k}^\beta}} e^{-j\phi_k}. \quad (30)$$

Now, we have that the channel gain can be expressed as follows:

$$\begin{aligned} E\{|h_S|^2\} &= E\left\{\left|\sqrt{\frac{\eta P_{S,B}}{L_B^\alpha}} \|\tilde{\mathbf{h}}_B\| + \sqrt{\eta N_G P_{S,G}} Ge^{-j\Omega}\right|^2\right\} \\ &= E\left\{\frac{\eta P_{S,B}}{L_B^\alpha} \|\tilde{\mathbf{h}}_B\|^2\right\} \\ &+ E\left\{\eta \sqrt{\frac{P_{S,B} N_G P_{S,G}}{L_B^\alpha}} \|\tilde{\mathbf{h}}_B\| G \cos(\Omega)\right\} \\ &+ E\{\eta N_G P_{S,G}\}. \end{aligned} \quad (31)$$

For the first term of (31), it is known that $E\{\|\tilde{\mathbf{h}}_B\|^2\} = N_B$ with $\tilde{\mathbf{h}}_B$ being the normalized channel coefficient, we have

$$E\left\{\frac{\eta P_{S,B}}{L_B^\alpha} \|\tilde{\mathbf{h}}_B\|^2\right\} = \frac{\eta N_B P_{S,B}}{L_B^\alpha}. \quad (32)$$

For the second term of (31), we can prove that Ω follows a uniform distribution over $(0, 2\pi)$, i.e., $\Omega \sim U(0, 2\pi)$, as follows.

- 1) Given a_1, a_2 , and two random variables ω_1 and ω_2 , which both follow uniform distributions over $(0, 2\pi)$, we can define a random variable (RV) $G_1 e^{j\Omega_1} = a_1 e^{j\omega_1} + a_2 e^{j\omega_2}$. Then we can define the RV $\hat{\Omega}_1 = \text{mod}(\Omega_1, 2\pi)$ with support on $(0, 2\pi)$.
- 2) Based on the properties of vector addition in a two-dimensional plane, we can conclude that the conditional probability density function (CPDF) of $\hat{\Omega}_1$ depends on the absolute difference between $\hat{\Omega}_1$ and ω_1 , thus its CPDF with ω_1 can be denoted as $f_{\hat{\Omega}_1, \omega_1}(\Phi) = F(\Delta\Phi)$, where $\Delta\Phi = \text{mod}(\Phi - \omega_1, 2\pi)$.
- 3) Note that for any given Φ , the range of $\Delta\Phi$ is $[0, 2\pi]$ when ω_1 varies in $[0, 2\pi]$. Based on the definition of PDF, we have $\int_0^{2\pi} F(\Delta\Phi) d\Phi = \int_0^{2\pi} F(\Delta\Phi) d\omega_1 = 1$. Since $\omega_1 \sim U(0, 2\pi)$, the PDF of $\hat{\Omega}_1$ can be given by

$$\begin{aligned} f_{\hat{\Omega}_1}(\Phi) &= \int_0^{2\pi} f_{\hat{\Omega}_1, \omega_1}(\Phi) \frac{1}{2\pi} d\omega_1 \\ &= \frac{1}{2\pi} \int_0^{2\pi} F(\Delta\Phi) d\omega_1 = \frac{1}{2\pi}. \end{aligned} \quad (33)$$

We thus proved that $\text{mod}(\Omega_1, 2\pi)$ follows a uniform distribution over $(0, 2\pi)$.

- 4) Set $G_k e^{j\Omega_k} = G_{k-1} e^{j\Omega_{k-1}} + a_{k+1} e^{j\omega_{k+1}}$ and repeat the above proof in step 1 ~ 3 for $k = 2, \dots, K-1$. We can prove that $G_{K-1} e^{j\Omega_{K-1}} = \sum_{k=1}^{K-1} a_k e^{j\omega_k}$ follows a uniform distribution over $(0, 2\pi)$.
- 5) Let $a_k = \sqrt{\frac{1}{L_{G,k}^\beta}}$ and $\omega_k = -\phi_k$. Combining with (30), it is proved that Ω follows a uniform distribution over $(0, 2\pi)$.

Therefore, we have that $E\{\cos(\Omega)\} = 0$. Furthermore, note that $\|\tilde{\mathbf{h}}_B\|$, G , and $\cos(\Omega)$ are uncorrelated, thus the second term of (31) is zero.

Now we move to the third term of (31). We start by proving the following equation:

$$E\{G^2\} = \sum_{k=1}^K \frac{1}{L_{G,k}^\beta} \quad (34)$$

which can be derived following the below calculations.

$$G e^{-j\Omega} = \sum_{k=1}^K \sqrt{\frac{1}{L_{G,k}^\beta}} \cos(\phi_k) - i \sum_{k=1}^K \sqrt{\frac{1}{L_{G,k}^\beta}} \sin(\phi_k), \quad (35)$$

$$G^2 = \left(\sum_{k=1}^K \sqrt{\frac{1}{L_{G,k}^\beta}} \cos(\phi_k) \right)^2 + \left(\sum_{k=1}^K \sqrt{\frac{1}{L_{G,k}^\beta}} \sin(\phi_k) \right)^2, \quad (36)$$

$$E\{G^2\} = \sum_{k=1}^K E\left\{ \frac{1}{L_{G,k}^\beta} \cos^2(\phi_k) \right\} + \sum_{k=1}^K E\left\{ \frac{1}{L_{G,k}^\beta} \sin^2(\phi_k) \right\}, \quad (37)$$

$$E\{G^2\} = \frac{1}{2} \sum_{k=1}^K \frac{1}{L_{G,k}^\beta} + \frac{1}{2} \sum_{k=1}^K \frac{1}{L_{G,k}^\beta} = \sum_{k=1}^K \frac{1}{L_{G,k}^\beta}, \quad (38)$$

where (38) is obtained follows from $\phi_k \sim U(0, 2\pi)$. Therefore, the third term of (31) is given by

$$E\left\{ \frac{\eta N_G}{(N_B + K)} G^2 \right\} = \frac{\eta N_G}{(N_B + K)} \sum_{k=1}^K \frac{1}{L_{G,k}^\beta}. \quad (39)$$

By summing (32) and (39), we can obtain

$$E\{|h_S|^2\} = \frac{\eta N_B P_{S,B}}{L_B^\alpha} + \eta N_G P_{S,G} \sum_{k=1}^K \frac{1}{L_{G,k}^\beta}. \quad (40)$$

By substituting $P_{S,B} = \frac{N_B}{N_B + K}$ and $P_{S,G} = \frac{1}{N_B + K}$ into (40), the average channel gain under the SD scheme can finally be obtained as

$$E\{|h_S|^2\} = \frac{\eta N_B^2}{L_B^\alpha (N_B + K)} + \frac{\eta N_G}{(N_B + K)} \sum_{k=1}^K \frac{1}{L_{G,k}^\beta}. \quad (41)$$

APPENDIX B

PROOF OF PROPOSITION 2

Let the downlink channel gain of waveguide RF port k be denoted as $p_k = \frac{\eta N_G}{L_{G,k}^\beta}$. Assume the total transmit power is 1, with the power allocation ratio for each port being w_k and $\sum_{k=1}^K w_k = 1$. According to Equation (4), the transmitted signals from all waveguides can be coherently combined at the receiver, resulting in an equivalent channel gain of $\left(\sum_{k=1}^K \sqrt{p_k w_k} \right)^2$. We then formulate the following optimization problem

$$\begin{aligned} \arg \max_{w_k} & \left(\sum_{k=1}^K \sqrt{p_k w_k} \right)^2 \\ \text{s.t.} & \sum_{k=1}^K w_k = 1, w_k \geq 0, \end{aligned} \quad (42)$$

which is a convex optimization problem. Using the method of Lagrange multipliers, we can conclude that the maximum channel gain $\sum_{k=1}^K p_k$ is achieved when the power allocation coefficients satisfy

$$w_k^* = \frac{p_k}{\sum_{k=1}^K p_k} = \frac{1}{\sum_{k=1}^K \frac{\eta N_G}{L_{G,k}^\beta}} \frac{\eta N_G}{L_{G,k}^\beta}. \quad (43)$$

APPENDIX C

PROOF OF PROPOSITION 3

The derivation of (18) is given as follows.

$$\begin{aligned} & E\{|h_C|^2\} \\ &= E\left\{ \left| \sqrt{\frac{\eta P_{C,B}}{L_B^\alpha}} \|\tilde{\mathbf{h}}_B\| + \sqrt{\eta P_{C,G} \sum_{k=1}^K \frac{N_G}{L_{G,k}^\beta}} e^{-j\phi_1} \right|^2 \right\} \\ &= \frac{\eta P_{C,B}}{L_B^\alpha} E\left\{ \|\tilde{\mathbf{h}}_B\|^2 \right\} \\ &+ E\left\{ \frac{\eta}{\sqrt{L_B^\alpha}} \sqrt{P_{C,B} P_{C,G} \sum_{k=1}^K \frac{N_G}{L_{G,k}^\beta}} \|\tilde{\mathbf{h}}_B\| \cos(\phi_1) \right\} \\ &+ \eta P_{C,G} \sum_{k=1}^K \frac{N_G}{L_{G,k}^\beta} \\ &= \frac{\eta N_B P_{C,B}}{L_B^\alpha} + \eta N_G P_{C,G} \sum_{k=1}^K \frac{1}{L_{G,k}^\beta} \end{aligned} \quad (44)$$

The last equality holds because $\phi_1 \sim U(0, 2\pi)$ and the cross-product term is zero. With $P_{S,B} = \frac{N_B}{N_B+K}$ and $P_{S,G} = \frac{1}{N_B+K}$, the average channel gain under the SD scheme is obtained as

$$E \left\{ |h_C|^2 \right\} = \frac{\eta N_B^2}{(N_B + K) L_B^\alpha} + \frac{\eta N_G K}{(N_B + K)} \sum_{k=1}^K \frac{1}{L_{G,k}^\beta}. \quad (45)$$

REFERENCES

- [1] G. J. Foschini, "Layered space-time architecture for wireless communication in a fading environment when using multi-element antennas," *Bell labs technical journal*, vol. 1, no. 2, pp. 41–59, 1996.
- [2] E. G. Larsson, O. Edfors, F. Tufvesson, and T. L. Marzetta, "Massive MIMO for next generation wireless systems," *IEEE Commun. Mag.*, vol. 52, no. 2, pp. 186–195, 2014.
- [3] M. Di Renzo, A. Zappone, M. Debbah, M.-S. Alouini, C. Yuen, J. De Rosny, and S. Tretyakov, "Smart radio environments empowered by reconfigurable intelligent surfaces: How it works, state of research, and the road ahead," *IEEE journal on selected areas in communications*, vol. 38, no. 11, pp. 2450–2525, 2020.
- [4] N. Shlezinger, G. C. Alexandropoulos, M. F. Imani, Y. C. Eldar, and D. R. Smith, "Dynamic metasurface antennas for 6G extreme massive MIMO communications," *IEEE Wireless Commun.*, vol. 28, no. 2, pp. 106–113, 2021.
- [5] W. K. New, K.-K. Wong, H. Xu, C. Wang, F. R. Ghadi, J. Zhang, J. Rao, R. Murch, P. Ramírez-Espinosa, D. Morales-Jimenez *et al.*, "A tutorial on fluid antenna system for 6G networks: Encompassing communication theory, optimization methods and hardware designs," *IEEE Commun. Surveys Tuts.*, 2024.
- [6] L. Zhu, W. Ma, and R. Zhang, "Movable antennas for wireless communication: Opportunities and challenges," *IEEE Commun. Mag.*, vol. 62, no. 6, pp. 114–120, 2023.
- [7] H. O. Y. Suzuki and K. Kawai, "Pinching antenna: Using a dielectric waveguide as an antenna," *NTT DOCOMO Technical J*, 2022.
- [8] Z. Yang, N. Wang, Y. Sun, Z. Ding, R. Schober, G. K. Karagiannidis, V. W. Wong, and O. A. Dobre, "Pinching antennas: Principles, applications and challenges," *arXiv preprint arXiv:2501.10753*, 2025.
- [9] Z. Ding and H. V. Poor, "LoS blockage in pinching-antenna systems: Curse or blessing?" *arXiv preprint arXiv:2503.08554*, 2025.
- [10] Y. Liu, Z. Wang, X. Mu, C. Ouyang, X. Xu, and Z. Ding, "Pinching antenna systems (pass): Architecture designs, opportunities, and outlook," *arXiv preprint arXiv:2501.18409*, 2025.
- [11] Z. Ding, R. Schober, and H. Vincent Poor, "Flexible-antenna systems: A pinching-antenna perspective," *IEEE Trans. Commun.*, pp. 1–1, 2025.
- [12] Y. Xu, Z. Ding, and G. K. Karagiannidis, "Rate maximization for downlink pinching-antenna systems," *IEEE Wireless Commun. Lett.*, 2025.
- [13] C. Ouyang, Z. Wang, Y. Liu, and Z. Ding, "Array gain for pinching-antenna systems (PASS)," *arXiv preprint arXiv:2501.05657*, 2025.
- [14] S. Hu, R. Zhao, Y. Liao, D. W. K. Ng, and J. Yuan, "Sum-rate maximization for pinching antenna-assisted NOMA systems with multiple dielectric waveguides," *arXiv preprint arXiv:2503.10060*, 2025.
- [15] M. Zeng, J. Wang, X. Li, G. Wang, O. A. Dobre, and Z. Ding, "Sum rate maximization for NOMA-assisted uplink pinching-antenna systems," *arXiv preprint arXiv:2505.00549*, 2025.
- [16] J. Zhang, H. Xu, C. Ouyang, Q. Zou, and H. Yang, "Uplink sum rate maximization for pinching antenna-assisted multiuser MISO," *arXiv preprint arXiv:2504.16577*, 2025.
- [17] A. Bereyhi, C. Ouyang, S. Asaad, Z. Ding, and H. V. Poor, "MIMO-PASS: Uplink and downlink transmission via MIMO pinching-antenna systems," *arXiv preprint arXiv:2503.03117*, 2025.
- [18] O. S. Badarneh, H. S. Silva, and Y. H. A. Badarneh, "Physical-layer security of pinching-antenna systems," *arXiv preprint arXiv:2503.18322*, 2025.
- [19] H. Jiang, Z. Wang, and Y. Liu, "Pinching-antenna system (pass) enhanced covert communications," *arXiv preprint arXiv:2504.10442*, 2025.
- [20] Z. Ding, "Pinching-antenna assisted ISAC: A CRLB perspective," *arXiv preprint arXiv:2504.05792*, 2025.
- [21] D. Bozanis, V. K. Papanikolaou, S. A. Tegos, and G. K. Karagiannidis, "Cramer-Rao bounds for integrated sensing and communications in pinching-antenna systems," *arXiv preprint arXiv:2505.01333*, 2025.
- [22] A. Khalili, B. Kaziu, V. K. Papanikolaou, and R. Schober, "Pinching antenna-enabled ISAC systems: Exploiting look-angle dependence of RCS for target diversity," 2025.
- [23] Z. Zhang, Y. Liu, B. He, and J. Chen, "Integrated sensing and communications for pinching-antenna systems (PASS)," *arXiv preprint arXiv:2504.07709*, 2025.
- [24] R. Heath, S. Peters, Y. Wang, and J. Zhang, "A current perspective on distributed antenna systems for the downlink of cellular systems," *IEEE Commun. Mag.*, vol. 51, no. 4, pp. 161–167, 2013.
- [25] A. Saleh, A. Rustako, and R. Roman, "Distributed antennas for indoor radio communications," *IEEE Trans. Commun.*, vol. 35, no. 12, pp. 1245–1251, 1987.
- [26] D. W. Group, "Design specification for distributed antenna systems," *Web Address: https://amta.org.au/business-and-industry/mobile-carriers-forum-mcf/in-building-coverage-information-for-property-owners-managers/*, 2023.
- [27] J. Wang, H. Wang, Y. Han, S. Jin, and X. Li, "Joint transmit beamforming and phase shift design for reconfigurable intelligent surface assisted MIMO systems," *IEEE Trans. Cognit. Commun. Networking*, vol. 7, no. 2, pp. 354–368, 2021.
- [28] C. Yi, W. Xu, Y. Sun, D. W. K. Ng, and Z. Wang, "Distributed multiuser precoding via unfolding WMMSE for multicell MIMO downlinks," *Early Access in IEEE Trans. Cognit. Commun. Networking*, 2024.
- [29] T. S. Rappaport, *Wireless communications: principles and practice*. Cambridge University Press, 2024.
- [30] B. S. Chaudhari and M. Zennaro, *LPWAN technologies for IoT and M2M applications*. Academic Press, 2020.
- [31] R. Corvaja and A. G. Armada, "Phase noise degradation in massive MIMO downlink with zero-forcing and maximum ratio transmission precoding," *IEEE Trans. Veh. Technol.*, vol. 65, no. 10, pp. 8052–8059, 2016.
- [32] Y. Zhang, J. Rong, J. Wu, X. Liu, Q. Xu, F. Tian, and Z. Zhang, "Evaluating EVM performance in millimeter-wave OTA test using digitally modulated stimuli with pre-distortion and a NVNA test bench," *IEEE Trans. Antennas Propag.*, vol. 73, no. 4, pp. 2271–2280, 2025.
- [33] S. Lv, Y. Liu, and Z. Ding, "Beam training for pinching-antenna systems (PASS)," *arXiv preprint arXiv:2502.05921*, 2025.